Growth of $In_xGa_{1-x}N$ and $In_xAl_{1-x}N$ on GaAs metalorganic molecular beam epitaxy

C. R. Abernathy, J. D. MacKenzie, S. R. Bharatan, K. S. Jones, and S. J. Pearton
Department of Materials Science and Engineering, University of Florida, Gainesville, Florida 32611

(Received 30 September 1994; accepted 24 October 1994)

$In_xGa_{1-x}N$ ($x=0.07$–1.0) and $In_xAl_{1-x}N$ ($x=0.16$–1.0) layers were grown on GaAs substrates by metalorganic molecular beam epitaxy. The films display strong *n*-type conductivity ($n>10^{20}$ cm^{-3}) for a wide range of InGaN compositions but only a limited range for InAlN films. The use of a H_2 rather than a He carrier gas produces a lower carrier concentration in the as-grown InGaN material. The surface morphology of the ternary layers is improved by the addition of Al to the surface while it is degraded by the addition of Ga. Nonetheless, the $In_xGa_{1-x}N$ is single crystal at low Ga concentrations with the lattice mismatch accommodated by a high density of stacking faults and microtwins. The InN layers contain only the cubic phase, while the ternaries contain both cubic and hexagonal phases.

The recent development of InGaN/GaN blue light-emitting diodes has intensified interest in the growth and properties of the wide band gap nitrides.[1] Several groups have reported stimulated emission from optically pumped InGaN/GaN heterostructures,[2,3] and a critical evaluation of the potential for wide band-gap compounds for high power electronic devices indicates that InGaN and related ternaries are well-suited for high-temperature operation.[4] Most of the $In_xGa_{1-x}N$ reported to date has been grown by metalorganic chemical vapor deposition (MOCVD) with device quality material generally being grown at ~800 °C.[1–3,5–7] There is interest in $In_xGa_{1-x}N$ grown by other techniques, including metalorganic molecular beam epitaxy (MOMBE), with the potential for more selective deposition or higher doping levels as found in MOMBE growth of other III–V materials. In this article we report the growth of $In_xGa_{1-x}N$ and $In_xAl_{1-x}N$ grown by MOMBE on (100)GaAs, paying particular attention to the variation of the structural and electrical properties with composition.

The samples were grown on semi-insulating, (100) GaAs substrates at 500 °C in an Intevac Gas Source Gen II. Triethylgallium (TEG) and trimethylindium (TMI) were transported by either H_2 or He carrier gases in order to examine possible hydrogen passivation effects, a common problem in organometallic vapor phase epitaxy grown GaN films.[8,9] Trimethylamine alane (TMAA) was used as the Al source for growth of the InAlN layers. An electron cyclotron resonance (ECR) plasma source (Wavemat MPDR 610) operating at 2.45 GHz and 200 W forward power was used to provide the nitrogen flux. Optical emission spectroscopy, shown in Fig. 1, indicates that a significant atomic nitrogen fraction is produced under these conditions though the presence of peaks at 335, 326, 390, and 391 nm shows there to be some N_2 and N_2^+ in the beam. The film compositions were varied by altering the relative group-III gas flow rates. Further details of the growth system have been given previously.[10]

The electrical transport properties of the ternary films were obtained from van der Pauw geometry Hall measurements at 300 K using alloyed (400 °C, 2 min) HgIn ohmic contacts. The composition of the InGaN samples was determined by electron microprobe analysis using a 6 keV beam. Surface morphology was examined by scanning electron microscopy (SEM) and cross-section transmission electron microscopy (TEM) was used for the defect analysis. Both x-ray diffraction (XRD) and selected area diffraction patterns (SADP) were used to distinguish between the wurtzite and zinc-blende phases.

Figure 2 shows the carrier concentration and mobility at room temperature in the $In_xGa_{1-x}N$ as a function of the experimentally determined In mole fraction. The pure InN grown with either H_2 or He carrier gas is strongly *n* type ($\sim 3\times10^{20}$ cm^{-3}). High *n*-type doping levels have also been observed in InN prepared by other methods. The source of this autodoping is usually ascribed to the presence of In vacancies,[11,12] though this seems less likely in light of the trends observed in InN grown using various V/III ratios.[10] The material retains carrier concentration above $\sim10^{20}$ cm^{-3} over the composition range InN to $\sim In_{0.2}Ga_{0.8}N$, at which point there is a sharp fall-off in the autodoping level. Note however, that the fall-off is more dramatic in material grown with the H_2 carrier gas, presumably due to hydrogen passivation of the defects responsible for the *n*-type conductivity. We have observed similar effects in InN films directly exposed to H_2 plasmas, where reduction in carrier concentra-

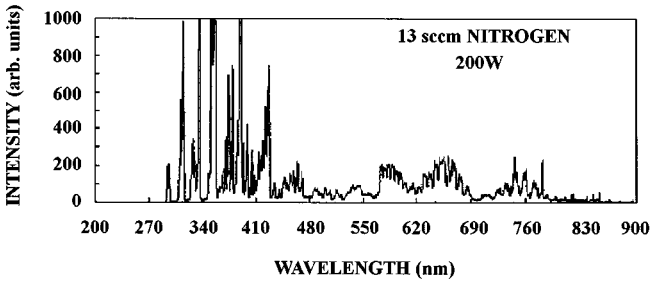

FIG. 1. Optical emission spectra taken from an N_2 plasma in the MOMBE-ECR source. N_2 flow was 13 sccm (cubic centimeters per min at standard temperature and pressure) and the microwave power was 200 W. Peaks at 326 and 335 nm indicate the presence of N_2 while those at 390 and 391 nm are due to N_2^+. The remaining peaks are due to N^+ and N.

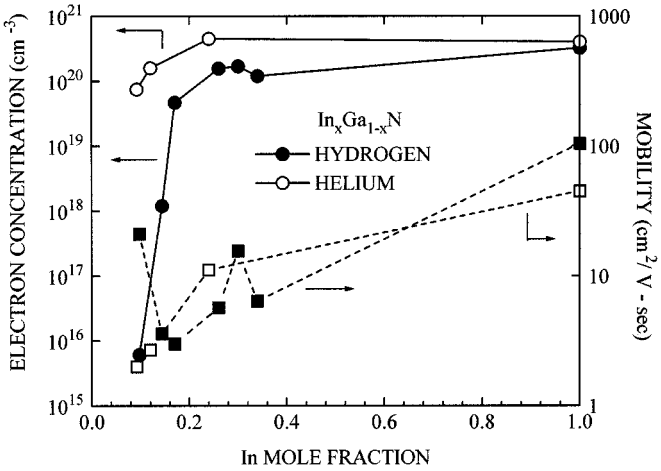

FIG. 2. Electron concentration and mobility at 300 K in $In_xGa_{1-x}N$ films grown at 500 °C on GaAs as a function of ternary composition. Compositions of $In_xGa_{1-x}N$ layers were determined by electronmicroprobe.

tion were measured when atomic hydrogen was incorporated into the material.[13] This suggests that hydrogen in any form, including molecular hydrogen, should be avoided during growth in order to avoid passivation of incorporated donors. As one would expect, the electron mobility generally decreases with decreasing In content in the $In_xGa_{1-x}N$, corresponding to increasing band gap.

InAlN layers grown using a H_2 carrier gas show a similar drop in n with decreasing In content (see Fig. 3) though the drop occurs at much higher values of X_{In}, $X_{In}\sim 0.7$ vs. 0.2. While this drop at higher In content is most likely due to the wider band gap of AlN relative to GaN, passivation of donors by the H_2 carrier gas must also be considered. To first order, however, it does appear that InAlN may be a more suitable cladding material unless the doping levels in the InGaN can be reduced substantially.

In Fig. 4, the top photograph shows an example of an InN layer grown using a low flux of TMI, such as is used for growth of InGaN. The surface clearly exhibits a platelet structure, unlike that normally observed for any of the other III–N grown by MOMBE under any conditions. It should be noted that this structure is not observed, and the morphology is specular, when higher TMI fluxes are used for the growth of InN. When TEG is added to the surface, along with the same flux of TMI as used in the top photograph, the surface takes on a rough appearance, which usually indicates the presence of a polycrystalline material with a very fine grain structure. GaN grown under the conditions used for the InGaN generally produces polycrystalline layers with morphologies similar to or worse than those shown in Fig. 4.

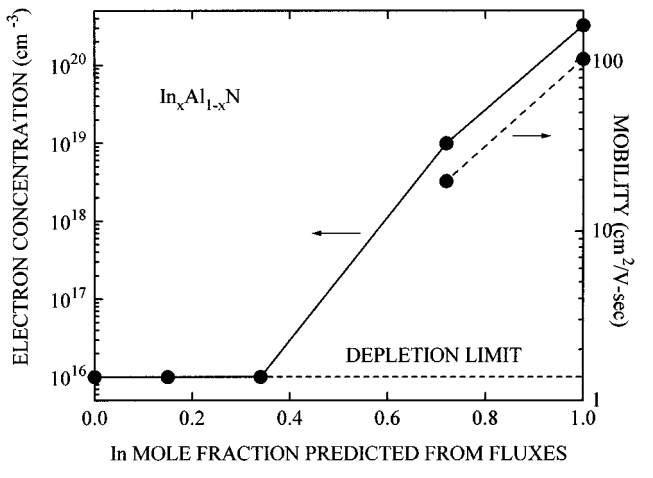

FIG. 3. Electron concentration and mobility at 300 K in $In_xAl_{1-x}N$ films as a function of ternary composition. Compositions of the $In_xAl_{1-x}N$ layers were estimated from the fluxes used and the growth rates of the respective binaries.

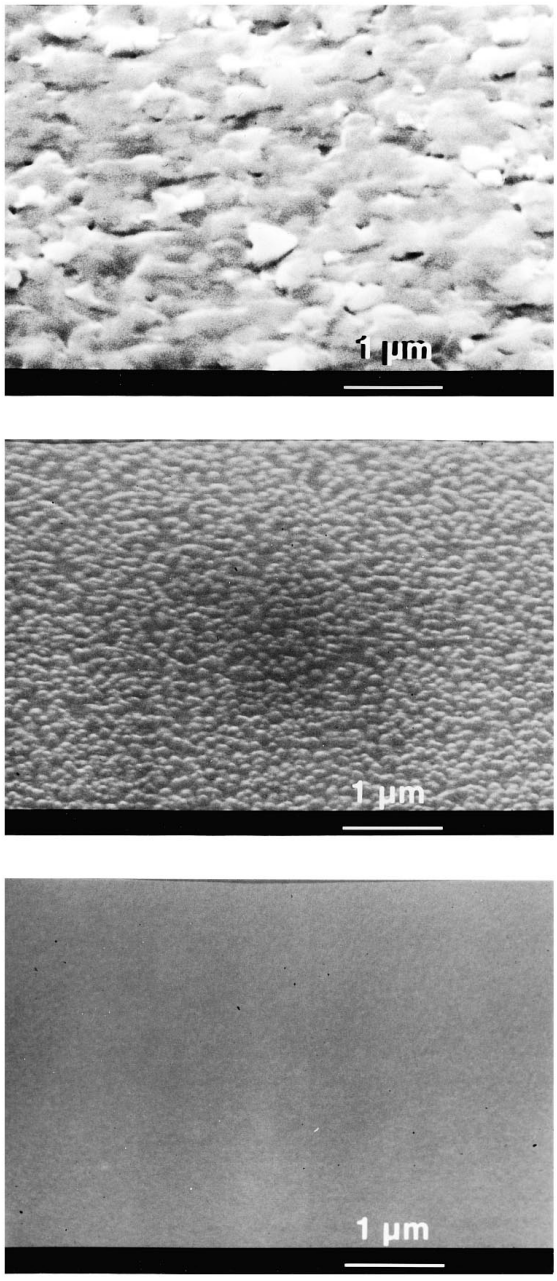

FIG. 4. SEM micrographs of InN (top), $In_{0.5}Ga_{0.5}N$ (middle), and $In_{0.35}Al_{0.65}N$ (bottom) layers grown on GaAs at 500 °C using the same TMI flow rates.

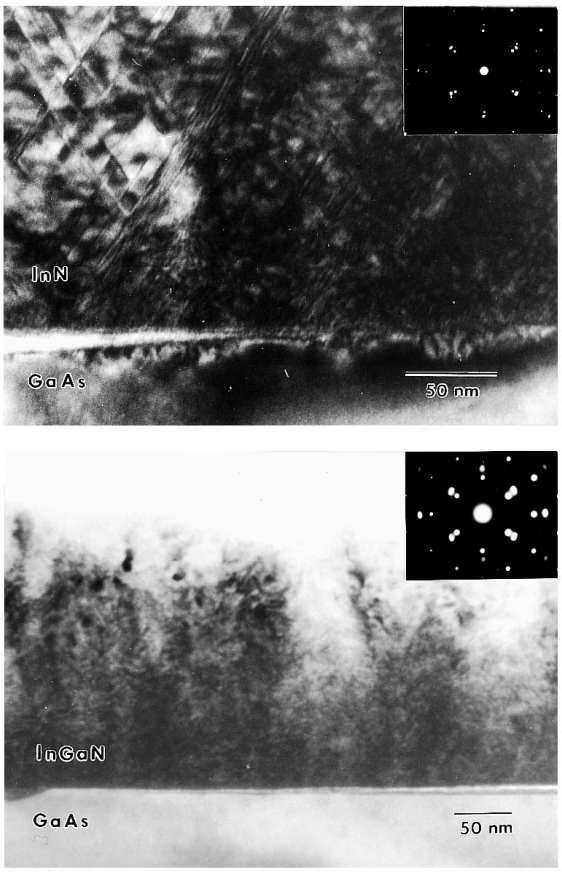

FIG. 5. Cross-section TEM micrographs and selected are diffraction patterns from InN (top) and $In_{0.26}Ga_{0.74}N$ (bottom) samples grown directly on GaAs. The TEM was performed under bright-field, **g**=[220] conditions.

Temperatures of ~700 °C are normally used to suppress this surface roughness. While higher temperatures may improve the surfaces of the InGaN layers with higher Ga content, the composition may become difficult to control due to desorption of In at $T>540$ °C. Further work is needed to determine the optimum growth temperatures in terms of morphology and reproducibility.

By contrast to the InGaN, the addition of Al to the surface improves the surface morphology, as shown at the bottom of Fig. 4. This is not surprising in light of the fact that AlN grown under similar conditions exhibits a specular surface. Apparently, higher growth temperatures are not required for good morphology in Al-containing compounds. This again suggests that InAlN may be a more suitable choice as a cladding layer since changes in growth temperature may not be required in order to achieve smooth surfaces.

XRD of the InGaN films showed that InN grown at a rate of 70 Å/min was cubic or β phase, while the ternaries contained both cubic and hexagonal or α phases. Since only (002)-type peaks from the film and substrate were visible in the θ–2θ powder diffractometer scans, this indicates the crystallographic orientation relationship is (001)GaAs$\|$(0001)α-$In_xGa_{1-x}N\|$(001)β-$In_xGa_{1-x}N$. Figure 5 (top) shows a bright field cross-sectional TEM micrograph of the InN layer obtained using two beam diffraction conditions with diffraction vector $g=[220]$ of the GaAs substrate. Stacking faults lying along the $\langle 111\rangle$ planes are the main defects present. The SADP of the epi–substrate region is shown in the upper right-hand corner of the micrograph, and using standard indexing methods the film–substrate orientation relationship was determined as (001)GaAs$\|$(001)β-InN and [011]GaAs$\|$[011]β-InN. The diffuse scattering visible in the SADP is due to the high stacking fault density in the InN. A cross-sectional TEM micrograph of an $In_{0.26}Ga_{0.74}N$ layer on GaAs is shown at the bottom of Fig. 5. The material is again defective single crystal and high-resolution microscopy showed that microtwins and stacking faults were the major structural imperfections. We observed qualitatively that the defect density was higher in the InGaN relative to InN, again suggesting that the growth temperature must be increased with increasing Ga content in order to maintain reasonable crystal quality.

In conclusion, we find strong n-type conductivity in $In_xGa_{1-x}N$ and $In_xAl_{1-x}N$ grown on GaAs by MOMBE. This conductivity is maintained in InGaN even at low In compositions. This autodoping is lower in samples grown with a H_2 carrier gas compared to samples grown with He, probably due to hydrogen passivation of the donor species. The InN layers are cubic single crystal, but contain a high density of stacking faults and microtwins due to the mismatch with the GaAs substrate.

Acknowledgments: The authors acknowledge the technical support of the staff of the Microfabritech facility at the University of Florida, and its director, Professor P. H. Holloway.

[1]S. Nakamura, T. Mukai, and M. Senoh, Appl. Phys. Lett. **64**, 1687 (1994).
[2]H. Amano, T. Tanaka, Y. Kunii, S. T. Kim, and I. Akasaki, Appl. Phys. Lett. **64**, 1377 (1994).
[3]M. Asif Khan, S. Krishnankutty, R. A. Skogman, J. N. Kuznia, D. T. Olson, and T. George, Appl. Phys. Lett. **65**, 520 (1994).
[4]T. P. Chow and R. Tyagi, IEEE Trans. Electron Devices **ED-41**, 1481 (1994).
[5]T. Maksuoka, T. Sasaki, and A. Katsui, Optoelectron. Dev. Technol. **5**, 53 (1990).
[6]N. Yoshimoto, T. Matsuoka, T. Sasaki, and A. Katsui, Appl. Phys. Lett. **59**, 2251 (1991).
[7]T. Nagamoto, T. Kuboyama, H. Minamino, and O. Omoto, Jpn. J. Appl. Phys. **28**, L1334 (1989).
[8]I. Akasaki, H. Amano, M. Kito, and K. Hiramatsu, J. Lumin. **68/49**, 666 (1991).
[9]S. Nakamura, M. Senoh, and T. Mukai, Jpn. J. Appl. Phys. **30**, L1708 (1991).
[10]C. R. Abernathy, P. Wisk, F. Ren, and S. J. Pearton, J. Vac. Sci. Technol. B **11**, 179 (1993).
[11]See, for example, S. Strite and H. Morkoç, J. Vac. Sci. Technol. B **10**, 1237 (1992).
[12]T. L. Tansley and C. P. Foley, Electron. Lett. **20**, 1066 (1984).
[13]S. J. Pearton, C. R. Abernathy, P. Wisk, W. S. Hobson and F. Ren, Appl. Phys. Lett. **63**, 1143 (1993).